Co-optimized bidding strategy of an integrated wind-thermal-photovoltaic system in deregulated electricity market under uncertainties

Co-optimized Bidding Strategy of an Integrated Wind-Thermal-Photovoltaic System in Deregulated Electricity Market Under Uncertainties

Hooman Khaloie[1], Amir Abdollahi[1], Miadreza Shafie-khah[2], Pierluigi Siano[3], Sayyad Nojavan[4], Amjad Anvari-Moghaddam[5], João P.S. Catalão[6]

(1) Department of Electrical Engineering, Shahid Bahonar University of Kerman, Kerman, Iran

(2) School of Technology and Innovations, University of Vaasa, 65200 Vaasa, Finland

(3) Department of Management & Innovation Systems, University of Salerno, Fisciano, Italy

(4) Department of Electrical Engineering, University of Bonab, Bonab, Iran

(5) Department of Energy Technology, Aalborg University, Aalborg, Denmark

(6) Faculty of Engineering of the University of Porto and INESC TEC, 4200-465, Porto, Portugal

---

Abstract

Clean Energy sources, such as wind and solar, have become an inseparable part of today's power grids. However, the intermittent nature of these sources has become the greatest challenge for their owners, which makes the bidding in the restructured electricity market more challenging. Hence, the main goal of this paper is to propose a novel multi-objective bidding strategy framework for a wind-thermal-photovoltaic system in the deregulated electricity market for the first time. Contrary to the existing bidding models, in the proposed model, two objective functions are taken into account that the first one copes with profit maximization while the second objective function concerns with emission minimization of thermal units. The proposed multi-objective optimization problem is solved using the weighted sum approach. The uncertainties associated with electricity market prices and the output power of renewable energy sources are characterized by a set of scenarios. Ultimately, in order to select the best-compromised solution among the obtained Pareto optimal solutions,

two diverse approaches are applied. The proposed bidding strategy problem is being formulated and examined in various modes of joint and disjoint operation of dispatchable and non-dispatchable energy sources. Simulation results illustrate that not only the integrated participation of these resources increases the producer's expected profit, but also decreases the amount of the produced pollution by the thermal units.

Keywords: Integrated operation, bidding strategy, Multi-objective optimization, Wind-thermal-Photovoltaic system, weighted-sum technique, Emission trading

---

Nomenclature

Indices

t	time index.
g	Index for thermal units.
ω	Scenario index.
b	Index for blocks of the generation cost curve and emission curve of thermal units.

Constants

π_ω	Probability of occurrence of scenario ω
$P^{W,Max}$	Rated wind power output, MW.
$P^{PV,Max}$	Rated PV power output, MW.
$STUC(g)$	Start-up cost of every thermal unit, €/each start-up.
$MDT(g)$	Minimum down-time of every thermal unit, hr.
$MUT(g)$	Minimum up-time of every thermal unit, hr.
$RUR(g)$	Ramp-up rate of every thermal unit, MW/hr.
$RDR(g)$	Ramp-down rate of every thermal unit, MW/hr.
E^{EQ}	Emission quota of power producer, lbs.

$P^{Maxb}(b,g)$	Maximum power output of every thermal unit in bth block of the piecewise linear cost function, MW.
$P^{Max}(g)$	Maximum power output of every thermal unit, MW.
$P^{Min}(g)$	Minimum power output of every thermal unit, MW.
$PS^{Max}(g)$	Maximum capacity of every thermal unit for participating in the spinning reserve market, MW.
$NC(g)$	No-load generating cost of every thermal unit, €/hr.
$IC(b,g)$	Incremental generating cost of bth block of unit g, €/MWhr.
$E(q,b,g)$	Slope of block b in emission group q of every thermal unit, lbs/MWhr.
EMG	Emission group including NO_X and SO_2.
$STURL(g)$	Start-up ramp bound of every thermal unit, MW/hr.
$STDRL(g)$	Shut-down ramp bound of every thermal unit g, MW/hr.
a_g, b_g, c_g	Coefficients of thermal generation cost function.
$\alpha_g, \beta_g, \gamma_g$	Emission coefficients of thermal unit g.
N_T	Number of periods.
N_G	Number of thermal units.
N_Ω	Number of scenarios.
N_b	Number of segments of the production cost and emission curve.
λ^{EM}	Emission market price, €/lbs.
Variables	
$\lambda^E(t,\omega)$	Price of day-ahead energy market, €/MW.
$\lambda^S(t,\omega)$	Price of spinning reserve market, €/MW.
$P^{th,S}(t,\omega)$	Optimal bid of thermal units in the spinning reserve market, MW.
$P^{th,E}(t,\omega)$	Optimal bid of thermal units in the day-ahead energy market, MW.
$P^W(t,\omega)$	Optimal bid of wind power plant in the day-ahead energy market, MW.
$P^{PV}(t,\omega)$	Optimal bid of PV system in the day-ahead energy market, MW.
$P^{th,Ac}(t,\omega)$	Actual power output of thermal units, MW.
$P^{W,F}(t,\omega)$	Realized power output of wind power plant, MW.
$P^{PV,F}(t,\omega)$	Realized power output of PV system, MW.
$P^C(t,\omega)$	Joint energy offer of the all energy resources in the day-ahead energy market, MW.

$\Delta^+(t,\omega)$	Imbalance-up, MW.
$\Delta^-(t,\omega)$	Imbalance-down, MW.
$STU(g,t,\omega)$	Start-up cost of every thermal unit, €.
$C(g,t,\omega)$	Generation cost of every thermal unit, €.
$EG(b,g,t,\omega)$	Produced power of thermal units through the bth block of the piecewise linear cost function for participating in the day-ahead energy market, MW.
$ES(g,t,\omega)$	Power offer of every thermal unit in the spinning reserve market, MW.
$ET(g,t,\omega)$	Total power offer by every thermal unit in all selected markets, MW.
$u(g,t,\omega)$	Binary variable which indicates acceptance situation of every thermal unit in the day-ahead energy market.
$x(g,t,\omega)$	Binary variable which indicates start-up situation of thermal units in the day-ahead energy market.
$y(g,t,\omega)$	Binary variable which indicates shut-down situation of thermal units in the day-ahead energy market.
$r^+(t,\omega)$	Imbalance penalty for over-generation as multiplier of energy price
$r^-(t,\omega)$	Imbalance penalty for under-generation as multiplier of energy price

1. Introduction

1.1. Motivation and Aim

Nowadays, a wide range of power system issues is affected by the presence of renewable energy resources. With the growth of industries and communities, the request for supplying customers demand is rising day-to-day [1]. In this regard, conventional energy sources such as coal, gas and nuclear, as well as renewable energy sources, e.g., hydro, wind and solar, are the two main options for governments to supply the required electricity of communities [2]. Generally, the rising cost of fossil fuels and attention to environmental concerns can be mentioned as the main reasons for the desire of diverse communities to augment the penetration of renewable energy sources [3]. Briefly, sustainability, environmentally friendly, reducing fossil fuel consumption, and low maintenance costs are

among the reasons for increasing the interest of various communities in renewable energy sources [4]. Despite many subsidies that governments have devoted to renewable energy developers, we will witness a significant increase in investments in this sector [5]-[6]. On the other hand, the existence of subsidies will not guarantee the profits of investors. Hence, the deregulated electricity market lay the groundwork for both producers and consumers to devise the best possible strategy for themselves. Consequently, renewable energy sources owned by generation companies (GenCos)/large consumers must design the most profitable bidding strategy by participating in various electricity markets.

1.2. Literature Review

The problem of optimal bidding strategy/self-scheduling has attracted the attention of many researchers so far [7]-[22]. A bidding structure based on the joint implementation of stochastic and robust uncertainty modeling approaches for an industrial consumer has been addressed in [7]. Likewise, in [8], the authors conducted a stochastic-robust optimization-based framework for a bidding strategy of a large consumer in a deregulated electricity market. In both papers [7] and [8], the uncertainty of load is addressed by the specified range, and the uncertainty related to renewable productions and market prices are modeled via independent scenarios. A self-scheduling model for the participation of a sample microgrid containing plug-in electric vehicles, wind turbines, and fuel cell units has been developed in [9]. In [10], authors have proposed a coordinated self-production and load-scheduling framework for an industrial plant in joint electricity and carbon emission markets. A hybrid probabilistic-possibilistic technique has been employed in [11] to cope with the uncertainties in the self-scheduling of thermal units. In [12], authors have focused on presenting a bi-objective self-scheduling structure for a typical factory as a large consumer. In [13], a risk-constrained self-scheduling model for a real virtual power plant in Iran has been suggested.

Integrated energy resources scheduling is one of the most challenging problems in the electrical power system which has attracted much attention. Wind

power generation as one of the most favorite organ of integrated energy resources has been widely considered alongside other production resources such as thermal, hydro, solar, and pumped storage power plants. In [14], the authors present an integrated self-scheduling model for a wind-pumped-storage system while the uncertainty of wind power generation is modeled by a neural network based technique. Authors illustrated that presenting a coordinated bidding strategy of both resources can remarkably raise their profitability. A critical shortage of this work is that the authors have not modeled the uncertainty associated with electricity market prices. Authors in [15], presented a linear programming framework for self-scheduling of a hydro-thermal system, whereas the electricity market prices and forced outages of generating units have been considered as uncertain sources. Likewise, the investigation of integrated wind and thermal energy sources in the context of the bidding strategy problem have been accomplished in [16]-[18]. The ultimate goal of all these three works is to prove the profitability of integrated scheduling compared to non-integrated one. In [19], a risk-based bidding framework for a wind-thermal-pumped storage system is presented.

Contrary to the mentioned studies, the bi-objective scheduling of integrated energy systems with the aim of minimizing pollution emission has also been considered by researchers [20]-[21]. In [20], a bi-objective microgrid self-scheduling model is presented in which the microgrid cost and emission minimizations are taking into account. A multi-objective self-scheduling model for a hydro-thermal system considering joint energy and ancillary services markets is proposed in [21]. In [22], a multi-objective economic dispatch model for pumped-hydro-thermal systems is presented in which the normal boundary intersection is utilized to achieve the Pareto optimal solutions. The taxonomy of reviewed papers [7]-[22] based on different aspects of their works has been listed in Table 1.

Table 1 is placed here

1.3. Contributions

According to the reviewed papers in subsection 1.2 and the specified characteristics for each paper in Table 1, this paper focuses on presenting a novel bi-objective bidding strategy of a wind-thermal-photovoltaic system in the energy and spinning reserve markets. To the best of authors' knowledge, this work proposes the most comprehensive study in the context of multi-objective and single-objective coordinated bidding strategy of wind, thermal and photovoltaic units in the literature, so the major contributions of this paper are:

- A comprehensive coordinated mathematical formulation is presented for the multi-objective bidding strategy of all existing sources.
- A novel bi-objective bidding strategy is proposed for a wind-thermal-photovoltaic (WTPV) system participating in the energy and spinning reserve markets. The process of profit maximization and emission minimization are concurrently accomplished while the uncertainty arising from day-ahead energy, spinning reserve, and imbalance prices along with the output power of renewable energy resources are addressed in the proposed framework.
- An efficient solution method, namely, the hybrid weighted sum method and fuzzy satisfying approach, is introduced as the solution methodology of the bi-objective bidding strategy problem
- A decision-making scheme based on the preferences of decision-maker is suggested in the bidding strategy problem to select the most favored solution.
- An additional pattern based on the emission trading concept is proposed for an emission-constrained WTPV power producer to select the best possible strategy.

2. Problem formulation

The multi-objective bidding strategy problem of a WTPV system is formulated as a stochastic mixed integer programming (MIP) which maximizing the expected profit of WTPV system and minimizing the expected emission arising from thermal units are considered as two distinct objective functions of the decision-maker. In the following subsections, separate objective functions of the bi-objective bidding strategy problem will be thoroughly explained.

2.1. First objective function: Maximizing expected profit

The primary purpose of the WTPV system is to maximize its profits through participation in diverse electricity markets in the 24-hour scheduled horizon. In the coordinated bidding structure, a single offering package will be offered to the energy market from all existing energy resources while the offering package of power producer in the spinning reserve market exclusively contains the participation of thermal units in this market. The first objective function of the power producer for the coordinated operation of all resources is formulated as follows:

$$\begin{aligned}\text{Max } F_1^C = & \sum_{\omega=1}^{N_\Omega} \pi_\omega \times [\sum_{t=1}^{T} (\lambda^E(t,\omega) P^{th,E}(t,w) + \lambda^E(t,\omega) P^W(t,w) \\ & + \lambda^E(t,\omega) P^{PV}(t,w) + \lambda^S(t,\omega) P^{th,S}(t,w) \\ & + \lambda^E(t,\omega) r^+(t,\omega) \Delta^+(t,\omega) - \lambda^E(t,\omega) r^-(t,\omega) \Delta^-(t,\omega))] \\ & - \sum_{\omega=1}^{N_\Omega} \pi_\omega \times [\sum_{t=1}^{T} \sum_{g=1}^{N_G} C(g,t,\omega) - \sum_{t=1}^{T} \sum_{g=1}^{N_G} (STU(g,t,\omega))] \end{aligned} \quad (1)$$

where the first two lines of (1) represent the expected income of power producer from participating in the day-ahead energy and spinning reserve markets while the third line relates to the imbalances of power producer in the balancing market, finally, the last line refers to the costs of operating and start-up costs of the thermal units. The constraints of the objective function (1) would be presented as follows:

$$0 \leq EG(b,g,t,\omega) \leq P^{Maxb}(b,g), \quad \forall b, \forall g, \forall t, \forall \omega \tag{2}$$

$$P^{Min}(g)u(g,t,\omega) \leq \sum_{b=1}^{N_b} EG(b,g,t,\omega) \leq P^{Max}(g)u(g,t,\omega), \quad \forall g, \forall t, \forall \omega \tag{3}$$

$$0 \leq ES(g,t,\omega) \leq PS^{Max}(g)u(g,t,\omega), \quad \forall g, \forall t, \forall \omega \tag{4}$$

$$P^{Min}(g)u(g,t,\omega) \leq ET(g,t,\omega) \leq P^{Max}(g)u(g,t,\omega), \quad \forall g, \forall t, \forall \omega \tag{5}$$

$$0 \leq P^{W}(t,\omega) \leq P^{W,Max}, \quad \forall t, \forall \omega \tag{6}$$

$$0 \leq P^{PV}(t,\omega) \leq P^{PV,Max}, \quad \forall t, \forall \omega \tag{7}$$

$$0 \leq STU(g,t,\omega) \geq STUC(g)x(g,t,\omega), \quad \forall g, \forall t, \forall \omega \tag{8}$$

$$\sum_{n=t-MUT(g)+1}^{t} x(g,t,\omega) \leq u(g,t,\omega), \quad \forall g, \forall t, \forall \omega \tag{9}$$

$$u(g,t,\omega) + \sum_{n=t-MDT(g)+1}^{t} y(g,t,\omega) \leq 1, \quad \forall g, \forall t, \forall \omega \tag{10}$$

$$\begin{aligned} \sum_{b=1}^{N_b} EG(b,g,t,\omega) \leq \sum_{b=1}^{N_b} EG(b,g,t-1,\omega) + RUR(g)u(g,t-1,\omega) \\ + STURL(g)x(g,t,\omega), \quad \forall g, \forall t > 1, \forall \omega \end{aligned} \tag{11}$$

$$\begin{aligned} \sum_{b=1}^{N_b} EG(b,g,t-1,\omega) \leq \sum_{b=1}^{N_b} EG(b,g,t,\omega) + RDR(g)u(g,t,\omega) \\ + STDRL(g)y(g,t,\omega), \quad \forall g, \forall t > 1, \forall \omega \end{aligned} \tag{12}$$

$$0 \leq \Delta^{+}(t,\omega) \leq P^{PV,F}(t,\omega) + P^{W,F}(t,\omega) + P^{th,Ac}(t,\omega), \quad \forall t, \forall \omega \tag{13}$$

$$0 \leq \Delta^{-}(t,\omega) \leq P^{PV,Max} + P^{W,Max} + \sum_{g=1}^{N_G} P^{Max}(g)u(g,t,\omega), \quad \forall t, \forall \omega \tag{14}$$

$$P^{C}(t,\omega) \leq P^{C}(t,\widetilde{\omega}), \quad \forall \omega, \widetilde{\omega} : [\lambda^{E}(t,\omega) \leq \lambda^{E}(t,\widetilde{\omega})], \quad \forall t \tag{15}$$

$$P^{th,S}(t,\omega) \leq P^{th,S}(t,\widetilde{\omega}), \quad \forall \omega, \widetilde{\omega} : [\lambda^{S}(t,\omega) \leq \lambda^{S}(t,\widetilde{\omega})], \quad \forall t \tag{16}$$

$$P^{C}(t,\omega) = P^{C}(t,\widetilde{\omega}), \quad \forall \omega, \widetilde{\omega} : [\lambda^{E}(t,\omega) = \lambda^{E}(t,\widetilde{\omega})], \quad \forall t \tag{17}$$

$$P^{th,S}(t,\omega) = P^{th,S}(t,\widetilde{\omega}), \quad \forall \omega, \widetilde{\omega} : [\lambda^{S}(t,\omega) = \lambda^{S}(t,\widetilde{\omega})], \quad \forall t \tag{18}$$

$$C(g,t,\omega) = NC(g)u(g,t,\omega) + \sum_{b=1}^{N_b} IC(b,g)EG(b,g,t,\omega), \quad \forall t, \forall \omega \tag{19}$$

$$\sum_{g=1}^{N_G}\sum_{b=1}^{N_b} EG(b,g,t,\omega) = P^{th,E}(t,\omega), \quad \forall t, \forall \omega \tag{20}$$

$$\sum_{g=1}^{N_G} ES(g,t,\omega) = P^{th,S}(t,\omega), \quad \forall t, \forall \omega \tag{21}$$

$$ET(g,t,\omega) = \sum_{b=1}^{N_b} EG(b,g,t,\omega) + ES(g,t,\omega), \quad \forall g, \forall t, \forall \omega \tag{22}$$

$$P^{C}(t,\omega) = P^{th,E}(t,\omega) + P^{W}(t,\omega) + P^{PV}(t,\omega) \quad \forall t, \forall \omega \tag{23}$$

$$\Delta(t,\omega) = P^{PV,F}(t,\omega) + P^{W,F}(t,\omega) + P^{th,Ac}(t,\omega) - P^{C}(t,\omega), \quad \forall t, \forall \omega \tag{24}$$

$$\Delta(t,\omega) = \Delta^{+}(t,\omega) - \Delta^{-}(t,\omega), \quad \forall t, \forall \omega \tag{25}$$

$$u(g,t-1,\omega)-u(g,t,\omega)+x(g,t,\omega)-y(g,t,\omega)=0,\quad \forall g,\forall t,\forall\omega \tag{26}$$

Inequalities (2) and (3) restrict the generated power of thermal units within their minimum and maximum bounds while constraint (4) is implemented to limit the spinning reserve offer of generation facility within their maximum capability in providing upward spinning reserve. Constraint (5) is fulfilled to restrict the total bids of thermal units in the day-ahead energy and spinning reserve market within their limited operating areas. Constraints (6) and (7) represent the upper and lower bounds of the scheduled power of renewable energy sources. Constraints (8) is fulfilled to calculate the start-up costs incurred by thermal units during the scheduling horizon. Other technical restrictions of thermal units, as well as the minimum up/down time are enforced by constraints (9)-(10). The ramp-up and ramp-down limitations, considering the shut-down and start-up ramps of thermal units are modeled by constraints (11)-(12). Restriction (13) limits the positive energy deviations of power producer within the total actual power output of all three sources while constraint (14) ensures that the negative energy deviations should not exceed the maximum capacity of renewable energy sources plus the maximum available capacity of thermal units. Constraints (15)-(16) and (17)-(18) are the non-decreasing and non-anticipativity settings for the offering packages in the energy and spinning reserve markets, respectively. The generation cost of thermal units for energy delivery is computed through constraint (19). The quadratic cost curve of thermal units makes the problem nonlinear. In order to overcome this issue, many researchers have been approximated this cost curve using various piecewise blocks [20]. In the current paper, these piecewise linearized segments are indexed by letter b. Constraint (20) represents the total bid of thermal units in the energy market. Equation (21) calculates total bid of thermal units in the spinning reserve market while equation (22) computes the total bid of thermal units in energy and spinning reserve markets. Coordinated operation constraints: Constraint (23) calculates the final bid of power producer that should be offered to the energy market. Constraints (24) and (25) model the imbalances of the power producer in the

balancing market. Finally, the logical relationship between the various status of thermal units is enforced by equality (26).

2.2. Second objective function: Minimizing expected emission

The second objective function of the power producer in the proposed structure is emission minimization. In fact, due to the worldwide rising concerns about environmental issues, minimizing the produced pollution by thermal units is consistently considered as one of the objective functions of the power producers in the optimization process. The linear form of this objective function would be as follows:

$$\text{Min} \;\; F_2^{th} = \sum_{\omega=1}^{N_\Omega} \pi_\omega \times [\sum_{q=1}^{EMG} \sum_{g=1}^{N_G} \sum_{b=1}^{N_b} E(q,b,g) EG(b,g,t,\omega)] \tag{27}$$

It is worth to note that in order to take advantage of linear programming in the proposed structure, the emission functions of thermal units, which generally have a quadratic form, are approximated by some piecewise linearized blocks. In the current paper, the SO_2 and NO_X are taken into consideration as the primary sources of emission [21].

In this paper, three different bidding strategies, including the coordinated and uncoordinated operation of various energy sources, are considered to thoroughly examine the productivity of the proposed structure. Fig. 1 shows these three different bidding strategies with their determinant constraints. These three trading strategies are designed to exhaustively assess the multi-objective bidding strategy problem based on the following modes of operation:

1. Uncoordinated operation of all three available energy resources.
2. Coordinated operation of two energy resources + Uncoordinated operation of the last energy resources.
3. Coordinated operation of all three available energy resources.

Note that the authors have passed up to present the formulation of the first and second trading strategies to avoid tautology in writing. It is notable that the superscript numbers in the constraints of the second strategy point out two distinct trading strategy in this case study.

Fig. 1 is placed here

2.3. Solution method of the multi-objective optimization problem

Most practical engineering issues are faced with more than one objective function, which in many cases, these objective functions conflict with each other. Multifarious techniques and methods have been employed in the literature to solve multi-objective problems, which ϵ-constraint technique [20] and the weighted sum (WS) approach [24] are among these methods. In the present paper, the weighted sum technique has been used to solve the multi-objective bidding strategy of wind-thermal-photovoltaic energy resources. In the weighted sum method, all objective functions with different weighting factors that represent the relative significance of each objective function are put together in a separate objective function according to the following equation:

$$\text{Min } [OF] = w_1 F_1^{'} + w_2 F_2 \tag{28}$$

subject to

$$\begin{cases} w_1 + w_2 = 1 \\ F_1^{'} = -F_1 \\ \text{All restrictions of the proposed probelm} \end{cases} \tag{29}$$

where F_1 and F_2 stand for the two conflicting objective functions of the proposed problem, i.e., profit maximization and emission minimization. One of the difficulties faced by decision-makers in the weighted sum method is the different scale of objective functions in (28). To this end, a fuzzy satisfying

approach is proposed to overcome this issue in the literature of multi-objective programming problems [21]. Based on this approach, the objective functions in (28) are normalized as follows:

$$\mathrm{F}_{1,\mathrm{pu}} = \frac{F_1 - F_1^{max}}{F_1^{max} - F_1^{min}} \tag{30}$$

$$\mathrm{F}_{2,\mathrm{pu}} = \frac{F_2^{max} - F_2}{F_2^{max} - F_2^{min}} \tag{31}$$

where $F_{1,pu}$ and $F_{2,pu}$ are the per unit values of objective functions F_1 and F_2, respectively. In fact, the equations (30) and (31) map the objective functions F_1 and F_2 in the range 0 and 1. (F_1^{max}, F_2^{max}) and $\left(F_1^{min}, F_2^{min}\right)$ represent the obtained maximum and minimum values of each objective function through the single objective optimization process, respectively. After normalizing each objective function, the objective function of the weighted sum method is rewritten as follows:

$$\text{Min } \ [OF] = w_1 \mathrm{F}_{1,\mathrm{pu}}^{'} + w_2 \mathrm{F}_{2,\mathrm{pu}} \tag{32}$$

2.4. Decision-maker's approach to select the best compromise solution

After obtaining the Pareto solutions via the WS method, the most favored solution among all set of solutions should be picked up. In the present paper, the final selection of the best compromise solution is accomplished based on the mindset, inclination, and preferences of decision-makers [25]. Indeed, decision-makers ascertain the minimum and maximum permissible values for the objective functions based on insight, the experience of previous years, short-term and long-term plans, and restrictions imposed by system operators. In this regard, for the objective function of maximizing profit, the minimum acceptable profit and for the objective function of minimizing emission, the maximum allowable emission is determined by the decision-maker, and finally, the most favored solution is selected based on these preconditions.

2.5. Uncertainty characterization

The uncertain sources in the optimal bidding strategy of a GenCo are generally divided into two groups: the price of various target markets and generation power of renewable energy sources. The methodology for modeling the uncertainties arising from electricity market prices and output power of renewable energy sources will be explained in the following subsections.

2.5.1. Market Prices uncertainty model

In the proposed framework, the normal probability density function (PDF) is utilized to model the three uncertain market prices: the day-ahead energy and spinning reserve market prices along with the real-time market price. The PDF of an electricity market price λ_{price} with mean μ_{price} and standard deviation σ_{price} would be formulated as follows:

$$f_{price}(\lambda_{price}, \mu_{price}, \sigma_{price}) = \frac{1}{\sigma_{price}\sqrt{2\pi}} exp\left[-\frac{(\lambda_{price} - \mu_{price})^2}{2\sigma_{price}^2}\right] \tag{33}$$

2.5.2. Wind power uncertainty model

As it is evident, the production power of a wind turbine is not constant and changes as a function of wind speed. In the current paper, the Weibull PDF has been considered for modeling wind speed. The Weibull PDF of wind speed V with scale and shape factors c and k is defined as follows:

$$f_{wind}(V, c, k) = \frac{k}{c}\left(\frac{V}{c}\right)^{k-1} exp\left[-\left(\frac{V}{c}\right)^{k}\right] \tag{34}$$

The generated power of a wind turbine in specified wind speed V has fully corresponded to its technical specifications, namely, cut-out speed v_{co}, cut-in speed v_{ci}, and rated speed v_r, which is calculated using the following equation:

$$P_{wind} = \begin{cases} 0, & 0 \le V \le v_{ci} \\ P_{rated} \times \left(\frac{V - v_{ci}}{v_r - v_{ci}}\right), & v_{ci} \le V \le v_r \\ P_{rated}, & v_r \le V \le v_{co} \end{cases} \tag{35}$$

2.5.3. Solar power uncertainty model

Solar irradiance is the most significant factor in determining the output power of photovoltaic units, which is always confronted with uncertainties. In this paper, the Beta PDF is utilized as an appropriate expression pattern of solar irradiance. The Beta PDF of solar irradiance Si is expressed as follows:

$$f_{irr}(Si,\alpha,\beta) = \begin{cases} \frac{\Gamma(\alpha+\beta)}{\Gamma(\alpha)\Gamma(\beta)} \times (Si)^{\alpha-1} \times (1-Si)^{\beta-1}, & 0 \le Si \le 1, \alpha \ge 0, \beta \ge 0 \\ 0, & otherwise \end{cases} \tag{36}$$

Given the solar irradiance Si of photovoltaic units, their efficiency η^{PV} and total area S^{PV}, the output power of PV units P_{PV} are calculated as follows [23]:

$$P_{PV} = \eta^{PV} \times S^{PV} \times Si \tag{37}$$

Finally, By assigning appropriate probability density functions to each uncertain parameter, scenarios associated with these parameters are constructed by the roulette wheel mechanism [23].

3. Emission trading

In this paper, a solution fits the purchasing or selling emission quotas is presented for those occasions that taking advantage of emission trading is accessible for GenCos/industrial consumers. In this regard, [26] and [27] have focused on the detailed investigation of emission trading pattern in China's container terminal and building materials industry, respectively. Based on this approach, after solving the multi-objective bidding strategy problem, a specific strategy for each Pareto optimal solution will be adopted. If the emission of thermal units per Pareto exceeds the emission quota, the GenCo will have to purchase additional emission quotas. However, if the emission of a GenCo in each Pareto is less than the assigned emission quota, the Genco can sell its surplus emission quota. As mentioned above, the total expected earnings of GenCo in every Pareto optimal solution will be calculated as follows:

$$TPF = EPP + \left[\lambda^{EM} \times \left(E^{EQ} - EEG\right)\right] \tag{38}$$

where the TPF is net expected profit, EPP is the expected profit of GenCo per Pareto, E^{EQ} is the assigned emission quota to GenCo, λ^{EM} refers to emission price, and the EEG stands for the expected emission of GenCo per Pareto. Ultimately, for each emission price, a Pareto with the maximum value of TEP is selected as the optimal Pareto solution of the proposed bidding strategy problem.

4. Results and discussion

4.1. Input data

The proposed system under study comprises five thermal units, a wind farm, and a PV site with the maximum capacity of 340 MW, 250 MW, and 150 MW for each, respectively. The economic and technical information on thermal units is provided in Table 2 and Table 3. These data have been extracted with some adjustments from [16]. Also, the data related to the emission curve of thermal units are given in Table 4. It is worthwhile to mention again that the quadratic cost and emission curves of thermal units are approximated by three piecewise blocks. This action, along with the proper formulation of the problem, leads to the absence of any nonlinear term in the proposed issue. On the basis of previously published papers, the SO_2 and NO_x are considered as the fundamental origins of emission [21]. The expected values of forecasted wind speed and solar irradiance [28] are portrayed in Fig. 2 while information on wind turbines and PV site are provided in Table 5.

Tables 2, 3, 4, and 5 are placed here

Figure 2 is placed here

In the proposed model, GenCo only allows the thermal units to participate in the spinning reserve market, and since the offer of each unit in this market has to be ready to deliver in ten minutes, the maximum offer for each unit in this market is calculated using $PS^{Max}(g) = \frac{1}{6} \times RUR(g)$ [29]. As outlined in subsection 2.5, five uncertainty sources exist in the proposed structure (day-ahead market, spinning reserve market, and imbalance prices as well as wind and PV generation). Based on the suggested model, for each parameter, the adequate number of scenarios based on the statistical analysis of [28] and [30] is constructed using roulette wheel mechanism, and with a common approach, i.e., fast forward reduction technique [16] and [19], the initially generated scenarios for each parameter are reduced to three representative scenarios. Consequently, the final scenario set will contain $3^5 = 243$ scenarios. The proposed structure is formulated based on the MIP and has been implemented in GAMS (general algebraic modeling system), with CPLEX as the solver.

4.2. Results

In order to assess the performance of the proposed structure, two different case studies are considered in this paper. In the first case study, we examine the single objective framework for the bidding strategy of the system under consideration, and in the second case study, the multi-objective bidding strategy of the wind-thermal-PV system is discussed. It is worth to note that in all case studies, the three trading strategies shown in Fig. 1 is fully explored. The first trading strategy appertained to the disjoint operation of all three energy sources in the electricity markets. The second trading strategy refers to the coordinated operation of wind and thermal units, while the PV system individually and independently participates in the electricity market. Eventually, the third trading strategy relates to the coordinated operation of all available energy sources.

4.2.1. Case study 1

As already mentioned, this case study focuses on the single objective bidding strategy of the system under study. In other words, this case study focuses solely on maximizing producer's profit without having a program or goal to minimize emissions. The results of this case study have been exhibited in Table 6. It is necessary to mention that this table will allow us to compare the economic and environmental aspects of different trading strategies. According to the obtained results, trading strategy 1 has the lowest expected profit (€302434.636) and the highest imbalance cost (€25369.536) among all three trading strategies. In contrast, coordinated operations of all three resources (trading strategy 3) have resulted in the highest profitability and the lowest imbalance cost, which the obtained results are €304509.778 and €15278.357, respectively. Similarly, in the second trading strategy that includes the coordinated operation of wind and thermal resources, more profit (€303221.192) and fewer imbalance cost (€23037.277) are obtained compared to the first strategy. From a different point of view, coordinated operation of energy resources in the proposed bidding strategy not only increase the profitability of the power producer but also reduces the emission of thermal units. It has to be noted that the numeric percent for comparing the decreasing or increasing values related to expected profit, expected emission, and expected imbalance cost of trading strategies two and three will be presented later to check out the effectiveness of the proposed bidding strategy.

Table 6 is placed here

Fig. 3 shows the expected participation of WTPV system in the energy and spinning reserve markets for all trading strategies. According to Fig. 3a, it is observed that at almost most of the hours, trading strategy 1 has more participation in the energy market. This issue has led the trading strategy 1 to have the highest imbalance cost, which ultimately leads to more reduction in the

expected profit of WTPV system. Besides, it can be viewed that the difference in the participation of various trading strategies in the day-ahead energy market reflects more during high market prices. On the other hand, as shown in Fig. 3b, the participation of WTPV system in the spinning reserve market for trading strategies 2 and 3 are similar at most hours. Also, the high day-ahead market prices during hours 11-14 have led to a reduction in producer's participation in the spinning reserve market for the specified time interval. In other words, the producer will have a greater willingness to participate in the energy market instead of participating in the spinning reserve market to gain more profit in the aforementioned time interval. Finally, Fig. 4 presents the comparison between the share of thermal units from the entire participation of WTPV system in the energy market for all trading strategies. The share of thermal units in trading strategies 1 and 2 are lower than the first trading strategy, which leads to lower emission of power producer, as reported in Table 6. It is worth mentioning that Fig. 3 and Fig. 4 are demonstrated to unfold how the coordinated trading strategy of various available sources will alter the expected participation of the whole system and thermal units in the energy and spinning reserve markets, respectively.

Figures 3 and 4 are placed here

4.2.2. Case study 2

This case study is designed to address the multi-objective bidding strategy of the wind-thermal-PV system. Contrary to the first case study, in this case study, minimizing the emission of thermal units is also added to one of the decision-maker's goals in the optimization process. As discussed in the previous sections, the weighted sum method is used to solve the multi-objective optimization problem. In this method, different weighting factors for objective functions (here, w1 and w2) are chosen subject to w1+ w2 = 1, and finally, the Pareto solutions of the proposed problem will be obtained. The results of Pareto for

trading Strategies 1, 2, and 3 are shown in Fig. 5, Fig. 6, and Fig. 7, respectively. Also, the normalized values of objective functions $F1$ and $F2$ in equations (30) and (31), i.e., $F_{1,pu}$ and $F_{2,pu}$, are reported in the aforementioned figures. These normalized values let us observe that the proposed bi-objective model can efficiently obtain various results in the range of 0 and 1 that do not agglutinate in a specific space and it is capable of covering almost any range of $F_{1,pu}$ and $F_{2,pu}$. After obtaining Pareto results, the proposed approach in subsection 2.4 is implemented to select the most favored solution among all Pareto solutions. The minimum and maximum predetermined limits for the profit and emission are assumed to be 20×10^3 lbs and € 250×10^3, respectively. It has to be noted that these limits are determined by the decision-maker (GenCo) to merely compare the results of different trading strategies under similar conditions and consequently, every other restriction can be imposed by the decision-maker. Accordingly, the presented Pareto solutions in Fig. 5, Fig. 6, and Fig. 7 will let us pick the most favored solution under different predetermined restrictions. The summary results of different trading strategies in terms of the environmental and economic evaluation of the multi-objective bidding strategy have been provided in Table 7. It is worth noting that the results of Table 7 correspond to the red box of Fig. 5, Fig. 6 and Fig. 7 ($P14$) that obtained through the suggested approach in subsection 2.4.

Table 7 is placed here

Figures 5, 6 and 7 are placed here

According to the provided results in Table 7, trading strategies 2 and 3 have also led to an increase in the producer's expected profit in the multi-objective bidding strategy. The expected profit for trading strategies one, two, and three is €253638.926, €255566.283, and €256978.704, respectively. In this regard, the most expected profit is achieved via the third trading strategy (€256978.704)

Which is consistent with the results of the previous case study. Similar to the first case study, in the second case study, the trading strategies 2 and 3 also diminish the imbalance costs and emissions in comparison with the first trading strategy.

Similar to Fig. 3, Fig. 8 illustrates the expected bids of power producer that are going to be submitted in the energy and spinning reserve markets for all three trading strategies. The expected production bids in the energy market (Fig. 8a) follow the explanation given about Fig. 3a, with the difference that the rates of production bids are significantly reduced. Fig. 8b allows us to conclude that the power producer's bidding approach in the spinning reserve market for all trading strategies will not affect the producer's strategy in this market. This issue stems from the fact that the producer tends to utilize the maximum level of participation in the spinning reserve market to gain its expected profit in whole trading strategies while the pollution constraints restrict its production in the energy market. At the remaining hours, the rising level of GenCo's participation in the energy market, the GenCo's involvement in the spinning reserve also increases. Analogous to Fig. 4, the comparison between the portion of thermal units from the total participation of the WTPV system in the energy market for all trading strategies in the multi-objective optimization approach is captured in Fig. 9. In fact, this figure exposes how the emission of both trading strategies 2 and 3 will be reduced in comparison with the first trading strategy. In comparison with the first case study, a large portion of the thermal units' production bids has been reduced, which is more evident in time intervals with lower energy prices.

Figures 8 and 9 are placed here

In order to participate in diverse electricity markets, the producers should submit their bidding packages to each specific market. The bidding curves of the power producer in the energy market for hours 8 and 22 for both single-objective and bi-objective bidding approaches are captured in Fig. 10 and Fig. 11. It can

be noticed that in the coordinated operation of energy resources, for example, trading strategy 3, a bidding curve from all three energy resources is submitted to the day-ahead energy market. As can be seen from these curves, the coordinated operation of two or all units (strategy 2 or 3) leads to a change in the producer's bidding curve compared to the uncoordinated one (strategy 1). This is evident for both single objective and bi-objective bidding approaches. Moreover, the drop in bid volumes of bi-objective bidding approach compared to the single objective one is noticeable as can be seen from these figures.

Figures 10 and 11 are placed here

In this paper, along with the proposed approach in subsection 2.4, emission trading is also taken into consideration as a new scheme in the decision-making process of the power producer. Following the explanations given in section 3, after solving the multi-objective bidding strategy problem and obtaining corresponding Pareto solutions, this approach is implemented to select the optimal solution among all Pareto solutions. The maximum TPF obtained by equation (38) will be the optimal solution corresponding to each emission price. One of the superiorities and advantages of this method versus other techniques is that the emission quota of the power producer is implicitly included in the bidding process. In the current paper, in order to avoid tautology in the demonstration of results, only the results of emission quota arbitraging for trading strategy 3 have been reported in Table 8. The emission quota of the power producer is considered 20×10^3 lbs. The bold numbers in each column pertaining to emission prices indicate the optimal Pareto solution for that particular emission price. As can be seen from this table, the increase in the price of emission leads to a reduction in the expected net profit of the power producer.

Table 8 is placed here

The final investigation of this paper is dedicated to examining the effect of

the number of scenarios on the principal output variables of the problem, i.e., expected profit and emission, and their standard deviation. To this end, different analyses under the different number of scenarios of operating variables, namely, renewable power productions and electricity market prices, are carried out, and results will be compared. It has to be noted that these analyses are conducted on the third trading strategy because of two reasons: first, the coordinated operation of wind, thermal, and PV units is selected as the final preferred bidding strategy and second, the third trading strategy involves one optimization problem where all existing uncertainty sources are present and, as a result, all uncertainties affect the outputs of the problem. The considered analyses are as follows:

1. Analysis 1: two representative scenarios for each uncertain parameter is considered in the scenario reduction stage. Consequently, the total number of scenarios in this analysis would be 2^5=32.

2. Analysis 2: three scenarios for each uncertain parameter is taken into account. The total number of scenarios is 3^5=243. In fact, this analysis is the same as the one proposed in this paper.

3. Analysis 3: the reduced number of scenarios for each uncertain parameter is equal to four, so the entire scenario set includes 4^5=1024 scenarios.

It is worth mentioning that the reduced scenarios are obtained according to provided descriptions in subsection 4.1. Fig. 12 and Fig. 13 demonstrate the attained expected profit and emission versus their standard deviations in various analyses. According to Fig. 12, raising the total number of scenarios will result in an increment in both expected profit and its standard deviation. On the contrary, based on Fig. 13, it can be observed that the expected emission of the system and its standard deviation will be reduced by moving toward larger scenario sets. In summary, enlarging scenario numbers will modify both expected profit and emission of the power producer, but it may seriously lead to a computational explosion. The results of the computation time for diverse

analyses have been depicted in Fig. 14. It can be seen from this figure that increasing the number of scenarios will considerably raise the solution time, especially in the bi-objective bidding approach. In this regard, by changing the attitude of the WTPV system from the second analysis to the third one in the case study 2, a 1% increase in the expected profit results in a 462% increment in the solution time. It has to be noticed that the scale of the vertical axis in Fig. 14 is logarithmic.

Figures 12, 13 and 14 are placed here

4.3. Discussion

In the current paper, a comprehensive bidding model for the participation of wind, thermal, and photovoltaic units has been proposed. In summary, by examining the presented results in two case studies using the suggested approach in subsection 2.4, we can conclude that the proposed trading strategies will increase the expected profit and reduce the expected emission of the power producer. In order to assess the effectiveness of the second and third trading strategies in comparison with the first trading strategy, Fig. 15 and Fig. 16 are provided. According to these figures, it can be concluded that:

1. In both case studies, the third trading strategy has the highest profit increment, which these values are 1.36% and 0.68% for the first and second case studies, respectively.

2. In both case studies of the second and third trading strategies, the emission of thermal units decreases compared to the first trading strategy, which is more striking in the first case study.

3. Trading strategy 3 has the highest imbalance reduction, especially in the bi-objective bidding approach.

4. Reducing the expected production bids in the energy market has led to a decrease in the cost of imbalances and, consequently, an increase in the producer's profit.

5. In the bi-objective bidding approach, the trading strategy of power producer will not affect the participation level of thermal units in the spinning reserve market.

Figures 15 and 16 are placed here

Nevertheless, the following directions are suggested for further research:

1. Considering a risk measuring index in the bi-objective bidding strategy of WTPV system as an additional parameter.

2. Proposing a bi-level bidding model for the WTPV system while it behaves as a price-maker producer in one of the target electricity markets.

5. Conclusion

In this paper, a new framework for multi-objective bidding strategy of an integrated wind-thermal-photovoltaic system alongside two different decision-making schemes was proposed to attain the introduced contributions. In order to assess the effectiveness of the suggested bidding structure, three different trading strategies, including coordinated and uncoordinated operation of generation units, along with their relevant formulation were comprehensively presented, and subsequently, an efficient technique was applied to solve the bi-objective problem.

The key findings of the suggested model are listed as follows:

1. The coordinated operation of all energy resources was led to the highest expected profit in both single-objective and multi-objective bidding strategies. In fact, in the bi-objective model, the aim was to evaluate the

profitability of the coordinated bidding strategy of all available sources in the presence of an additional objective function, which in this occasion, the proposed bidding strategy was also able to gain the total expected profit of the system.

2. The reduction in the output power of thermal units in the bi-objective approach will lead to considerable imbalance reduction in comparison with the single-objective one. This imbalance reduction was accompanied by a decrease in the participation of the system in the energy market.

3. The variation in the trading approach of the system in the bi-objective model did not affect the bidding decisions in the spinning reserve market.

4. The emission trading mechanism can be used as a beneficial pattern by the power producers to increase their profitability as the presented model in this paper results in higher values of expected profit for all emission prices lower than 1 €/lbs.

5. The greater scenario sets result in higher values of expected profit and its standard deviation while the expected emission and its standard deviation are reduced. In this regard, a slight variation in the fundamental output variables of the problem, i.e., expected profit and expected emission, by increasing the total number of scenarios will lead to a computational explosion.

References

[1] De Andrade Guerra, J.B.S.O., Dutra, L., Schwinden, N.B.C., Andrade, S.F. De, 2015. Future scenarios and trends in energy generation in Brazil: Supply and demand and mitigation forecasts. J. Clean. Prod. https://doi.org/10.1016/j.jclepro.2014.09.082

[2] Ram, M., Child, M., Aghahosseini, A., Bogdanov, D., Lohrmann, A., Breyer, C., 2018. A comparative analysis of electricity generation costs from

renewable, fossil fuel and nuclear sources in G20 countries for the period 2015-2030. J. Clean. Prod. 199, 687–704.

[3] Wesseh, P.K., Lin, B., 2017. Options for mitigating the adverse effects of fossil fuel subsidies removal in Ghana. J. Clean. Prod. https://doi.org/10.1016/j.jclepro.2016.09.214

[4] Zafar, M.W., Shahbaz, M., Hou, F., Sinha, A., 2019. From nonrenewable to renewable energy and its impact on economic growth: The role of research & development expenditures in Asia-Pacific Economic Cooperation countries. J. Clean. Prod. https://doi.org/10.1016/j.jclepro.2018.12.081

[5] Yin, G., Zhou, L., Duan, M., He, W., Zhang, P., 2018. Impacts of carbon pricing and renewable electricity subsidy on direct cost of electricity generation: A case study of China's provincial power sector. J. Clean. Prod. https://doi.org/10.1016/j.jclepro.2018.09.108

[6] Nie, P. yan, Chen, Y. hua, Yang, Y. cong, Wang, X.H., 2016. Subsidies in carbon finance for promoting renewable energy development. J. Clean. Prod. https://doi.org/10.1016/j.jclepro.2016.08.083

[7] Shi, X., Dini, A., Shao, Z., Jabarullah, N.H., 2019. Impacts of photovoltaic/wind turbine/microgrid turbine and energy storage system for bidding model in power system. J. Clean. Prod.

[8] Abedinia, O., Zareinejad, M., Doranehgard, M.H., Fathi, G., Ghadimi, N., 2019. Optimal offering and bidding strategies of renewable energy based large consumer using a novel hybrid robust-stochastic approach. J. Clean. Prod. 215, 878–889.

[9] Aliasghari, P., Mohammadi-Ivatloo, B., Alipour, M., Abapour, M., Zare, K., 2018. Optimal scheduling of plug-in electric vehicles and renewable micro-grid in energy and reserve markets considering demand response program. J. Clean. Prod. https://doi.org/10.1016/j.jclepro.2018.03.058

[10] Tan, M., Chen, Y., Su, Y. xin, Li, S. hu, Li, H., 2019. Integrated optimization model for industrial self-generation and load scheduling with tradable carbon emission permits. J. Clean. Prod. https://doi.org/10.1016/j.jclepro.2018.11.005

[11] Khaloie, H., Abdollahi, A., Rashidinejad, M., Siano, P., 2019. Risk-based probabilistic-possibilistic self-scheduling considering high-impact low-probability events uncertainty. Int. J. Electr. Power Energy Syst. 110, 598–612. https://doi.org/10.1016/j.ijepes.2019.03.021

[12] Perković, L., Mikulčić, H., Duić, N., 2018. Multi-objective optimization of a simplified factory model acting as a prosumer on the electricity market. J. Clean. Prod. https://doi.org/10.1016/j.jclepro.2016.12.078

[13] Hooshmand, R.A., Nosratabadi, S.M., Gholipour, E., 2018. Event-based scheduling of industrial technical virtual power plant considering wind and market prices stochastic behaviors - A case study in Iran. J. Clean. Prod. https://doi.org/10.1016/j.jclepro.2017.12.017

[14] Varkani, A.K., Daraeepour, A., Monsef, H., 2011. A new self-scheduling strategy for integrated operation of wind and pumped-storage power plants in power markets. Appl. Energy 88, 5002–5012. https://doi.org/10.1016/j.apenergy.2011.06.043

[15] Esmaeily, A., Ahmadi, A., Raeisi, F., Ahmadi, M.R., Esmaeel Nezhad, A., Janghorbani, M., 2017. Evaluating the effectiveness of mixed-integer linear programming for day-ahead hydro-thermal self-scheduling considering price uncertainty and forced outage rate. Energy 122, 182–193. https://doi.org/10.1016/j.energy.2017.01.089

[16] Al-Awami, A.T., El-Sharkawi, M.A., 2011. Coordinated trading of wind and thermal energy. IEEE Trans. Sustain. Energy 2, 277–287. https://doi.org/10.1109/TSTE.2011.2111467

[17] Lakshmi, K., Vasantharathna, S., 2014. Gencos wind–thermal scheduling problem using Artificial Immune System algorithm. Int. J. Electr. Power Energy Syst. 54, 112–122. https://doi.org/10.1016/j.ijepes.2013.06.036

[18] Laia, R., Pousinho, H.M.I., Melíco, R., Mendes, V.M.F., 2016. Bidding strategy of wind-thermal energy producers. Renew. Energy 99, 673–681. https://doi.org/10.1016/j.renene.2016.07.049

[19] Al-Swaiti, M.S., Al-Awami, A.T., Khalid, M.W., 2017. Co-optimized trading of wind-thermal-pumped storage system in energy and regulation markets. Energy 138, 991–1005. https://doi.org/10.1016/j.energy.2017.07.10

[20] Aghaei, J., Alizadeh, M.I., 2013. Multi-objective self-scheduling of CHP (combined heat and power)-based microgrids considering demand response programs and ESSs (energy storage systems). Energy 55, 1044–1054. https://doi.org/10.1016/j.energy.2013.04.048

[21] Ahmadi, A., Aghaei, J., Shayanfar, H.A., Rabiee, A., 2012. Mixed integer programming of multiobjective hydro-thermal self scheduling. Appl. Soft Comput. J. 12, 2137–2146. https://doi.org/10.1016/j.asoc.2012.03.020

[22] Simab, M., Javadi, M.S., Nezhad, A.E., 2018. Multi-objective programming of pumped-hydro-thermal scheduling problem using normal boundary intersection and VIKOR. Energy 143, 854–866. https://doi.org/10.1016/j.energy.2017.09.144

[23] Soltani, S., Rashidinejad, M., Abdollahi, A., 2017. Stochastic Multiobjective Distribution Systems Phase Balancing Considering Distributed Energy Resources. IEEE Syst. J. https://doi.org/10.1109/JSYST.2017.2715199

[24] Jannati, J., Nazarpour, D., 2019. Optimal performance of electric vehicles parking lot considering environmental issue. J. Clean. Prod. 206, 1073–1088.

[25] Zakariazadeh, A., Jadid, S., Siano, P., 2014. Stochastic multi-objective operational planning of smart distribution systems considering demand response programs. Electr. Power Syst. Res. 111, 156–168.

[26] Zhong H, Hu Z, Yip TL. Carbon emissions reduction in China's container terminals: Optimal strategy formulation and the influence of carbon emissions trading. J Clean Prod 2019;219:518–30.

[27] Zhao, S., Shi, Y., Xu, J., 2018. Carbon emissions quota allocation based equilibrium strategy toward carbon reduction and economic benefits in China's building materials industry. J. Clean. Prod. 189, 307–325.

[28] Weather history+ - meteoblue [WWW Document], n.d. URL https://www.meteoblue.com/en/historyplus (accessed 4.22.19).

[29] Khaloie, H., Abdollahi, A., Rashidineiad, M., 2018. Risk-Constrained Self-Scheduling and Forward Contracting Under Probabilistic-Possibilistic Uncertainties, in: Electrical Engineering (ICEE), Iranian Conference On. IEEE, pp. 1138–1143. https://doi.org/10.1109/ICEE.2018.8472668.

[30] Bienvenido — ESIOS electricidad · datos · transparencia [WWW Document], n.d. URL https://www.esios.ree.es/es (accessed 3.14.19).

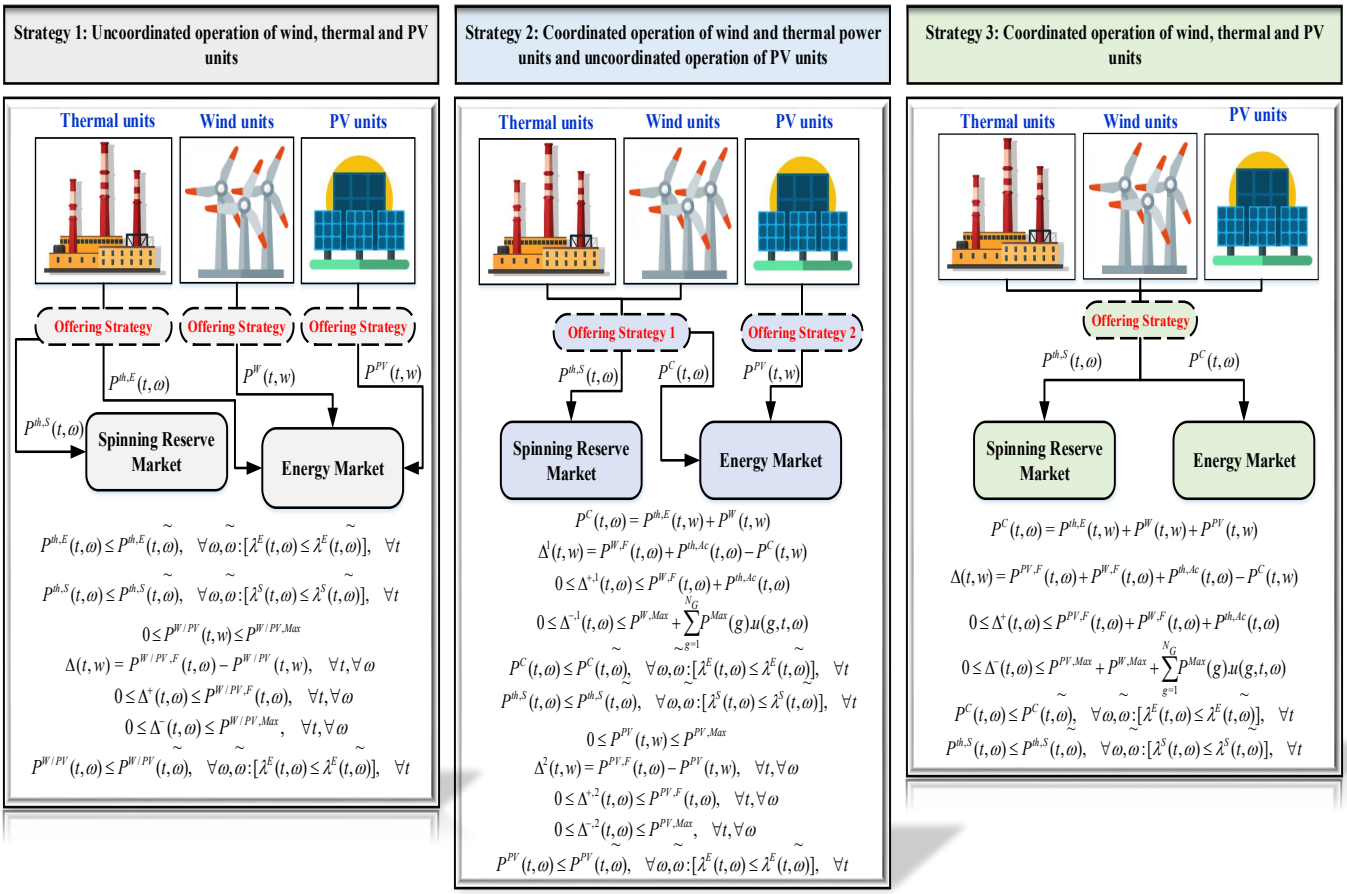

Figure 1: Schematic of different bidding strategies

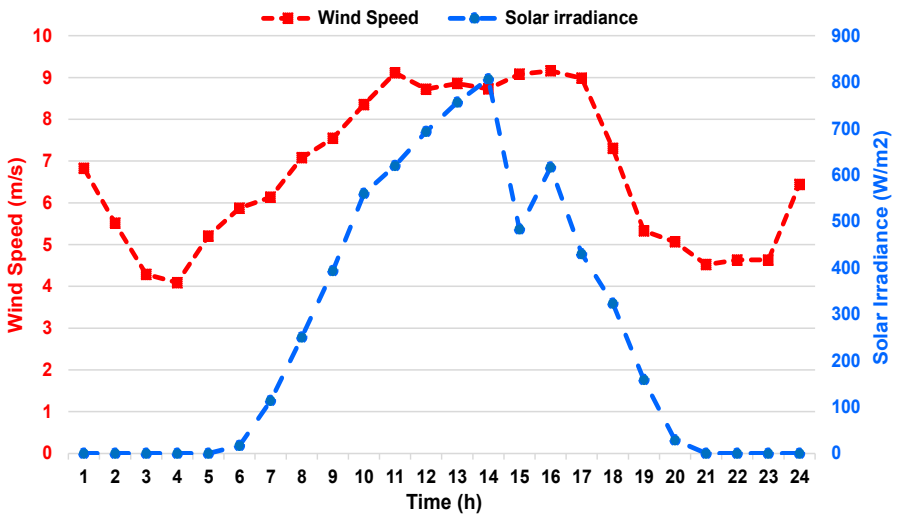

Figure 2: Expected values for hourly wind speed and solar irradiance

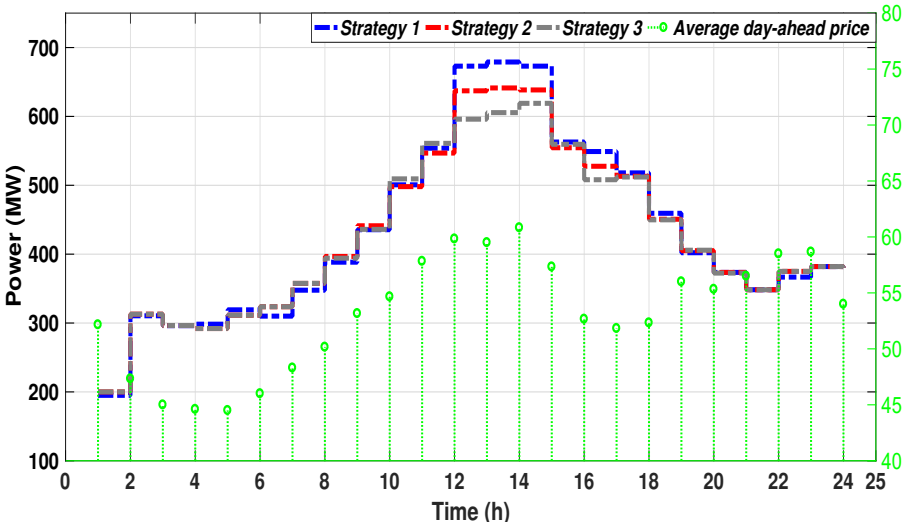

(a) Expected participation in the day-ahead energy market in different trading strategies

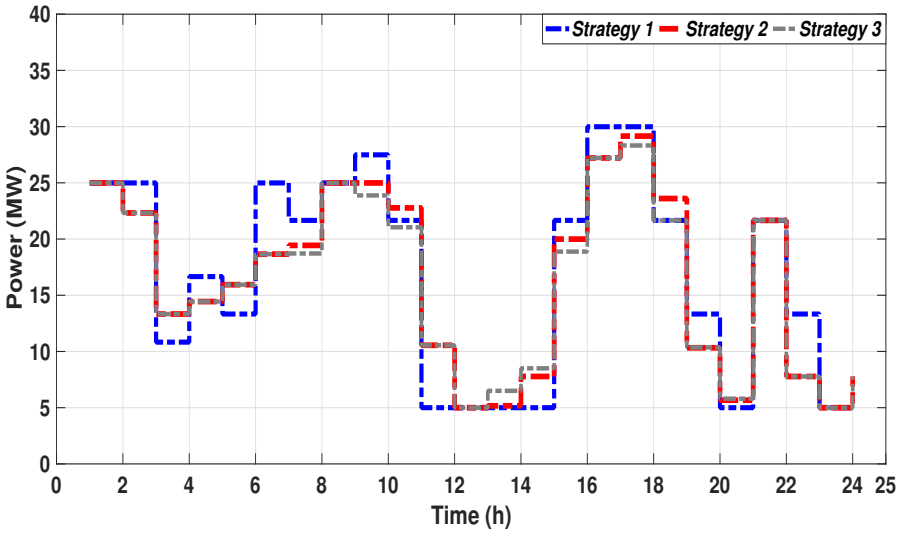

(b) Expected participation in the spinning reserve market in different trading strategies

Figure 3: Single objective bidding approach

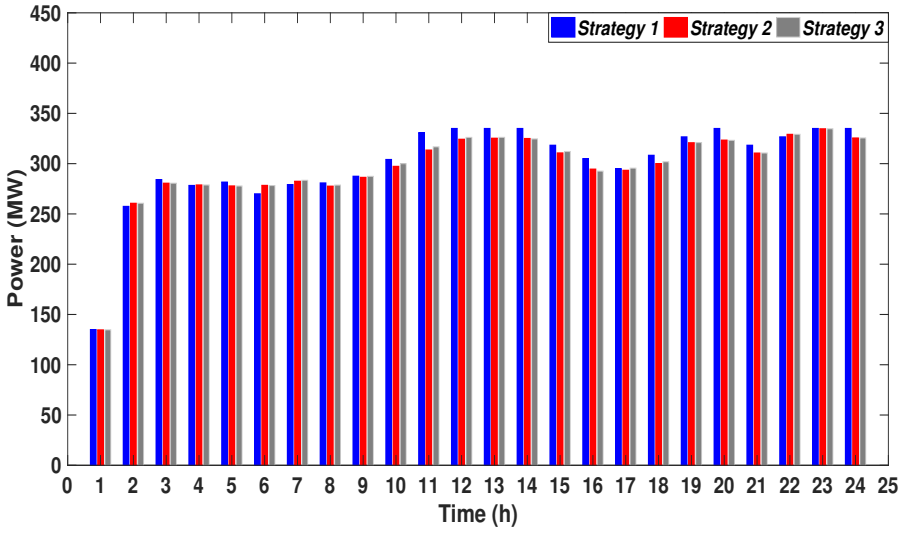

Figure 4: Comparison of expected amount of production bids of thermal units in the day-ahead energy market for all trading strategies (case study 1)

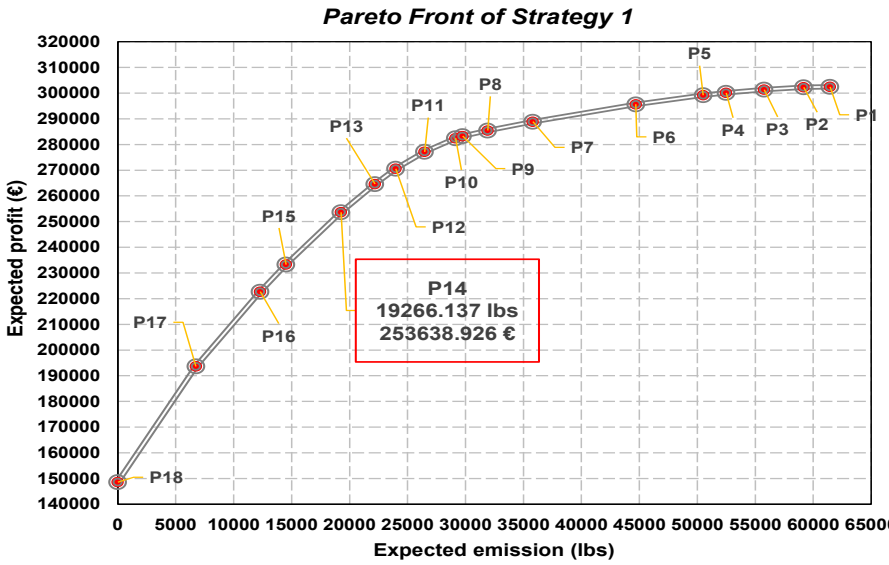

	P1	P2	P3	P4	P5	P6	P7	P8	P9
$F_{1,pu}$	1	0.9990	0.9929	0.9847	0.9787	0.9556	0.9117	0.8896	0.8754
$F_{2,pu}$	0	0.0370	0.0925	0.1459	0.1780	0.2726	0.4173	0.4805	0.5158
	P10	P11	P12	P13	P14	P15	P16	P17	P18
$F_{1,pu}$	0.8700	0.8356	0.7927	0.7541	0.6827	0.5503	0.4818	0.2927	0
$F_{2,pu}$	0.5257	0.5691	0.6097	0.6388	0.6865	0.7638	0.8001	0.8902	1

Figure 5: Pareto front for trading strategy 1

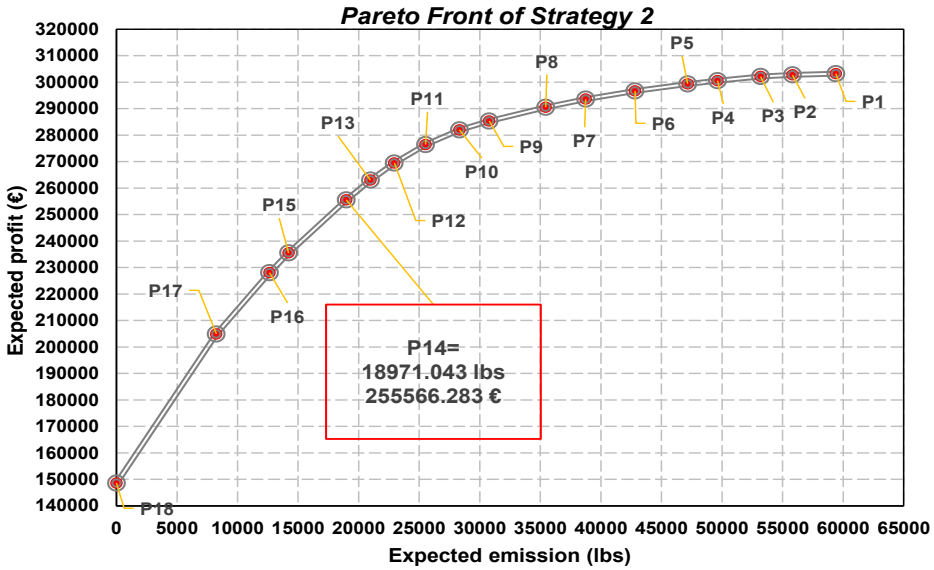

	P1	P2	P3	P4	P5	P6	P7	P8	P9
$F_{1,pu}$	1	0.9968	0.9928	0.9831	0.9750	0.9575	0.9375	0.9180	0.8843
$F_{2,pu}$	0	0.0603	0.1045	0.1645	0.2059	0.2791	0.3478	0.4034	0.4819
	P10	P11	P12	P13	P14	P15	P16	P17	P18
$F_{1,pu}$	0.8626	0.8268	0.7817	0.7397	0.6917	0.5622	0.5139	0.3640	0
$F_{2,pu}$	0.5231	0.5703	0.6138	0.6469	0.6806	0.7606	0.7872	0.8610	1

Figure 6: Pareto for trading strategy 2

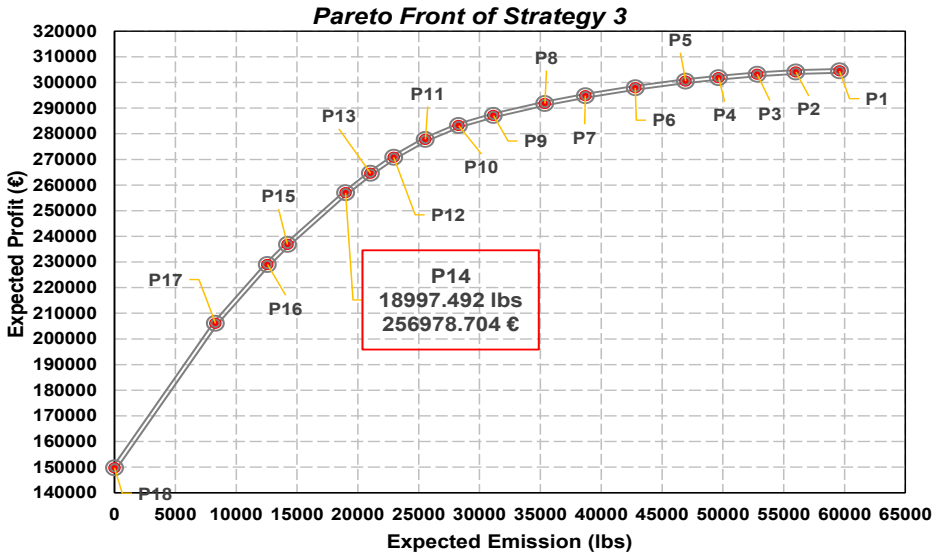

	P1	P2	P3	P4	P5	P6	P7	P8	P9
$F_{1,pu}$	1	0.9970	0.9914	0.9828	0.9742	0.9572	0.9372	0.9177	0.8874
$F_{2,pu}$	0	0.0600	0.1136	0.1667	0.2122	0.2816	0.3505	0.4063	0.4773
	P10	P11	P12	P13	P14	P15	P16	P17	P18
$F_{1,pu}$	0.8621	0.8272	0.7824	0.7418	0.6929	0.5627	0.5121	0.3637	0
$F_{2,pu}$	0.5253	0.5713	0.6148	0.6468	0.6811	0.7613	0.7891	0.8606	1

Figure 7: Pareto front for trading strategy 3

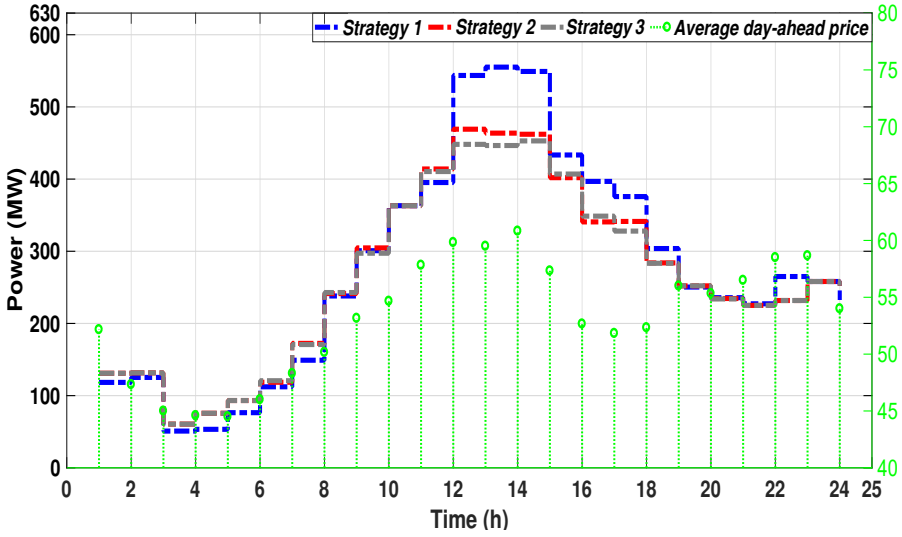

(a) Expected participation in the day-ahead energy market in different trading strategies

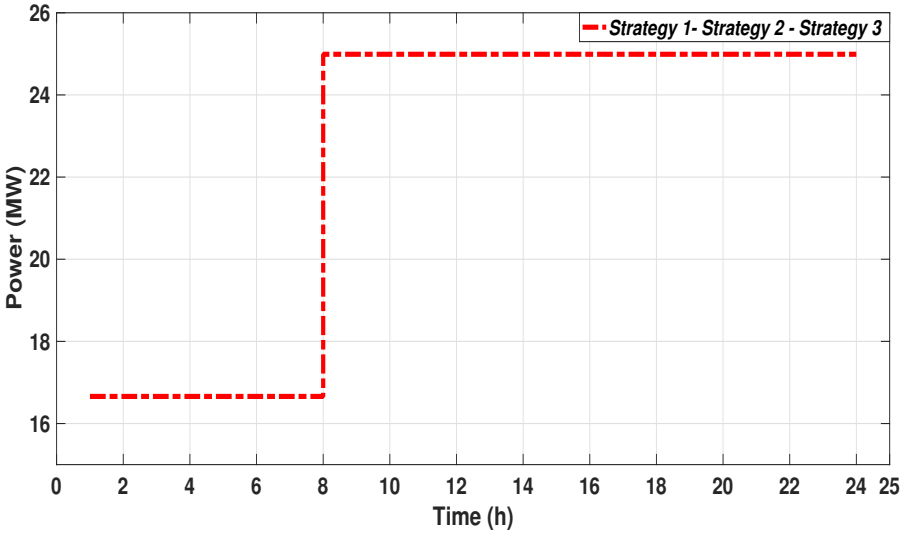

(b) Expected participation in the spinning reserve market in different trading strategies

Figure 8: Multi-objective bidding approach

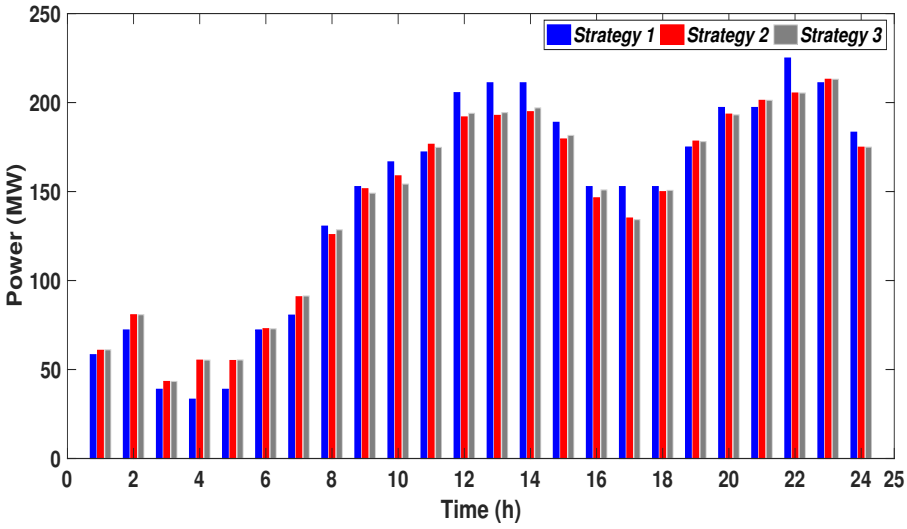

Figure 9: Comparison of expected amount of production bids of thermal units in the day-ahead energy market for all trading strategies (case study 2)

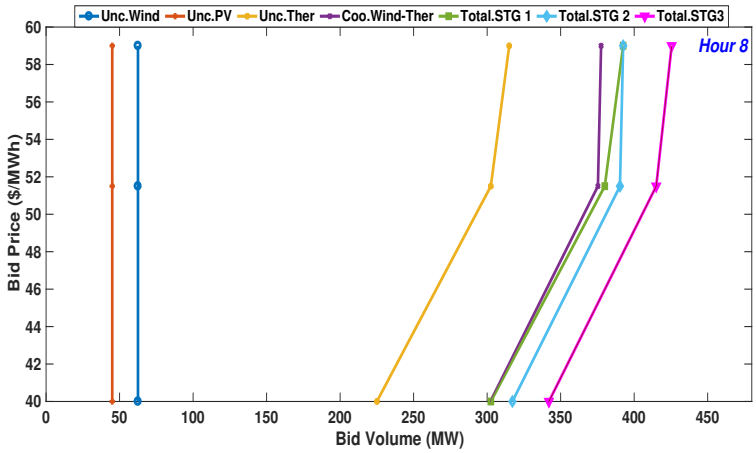

(a) Single objective bidding approach

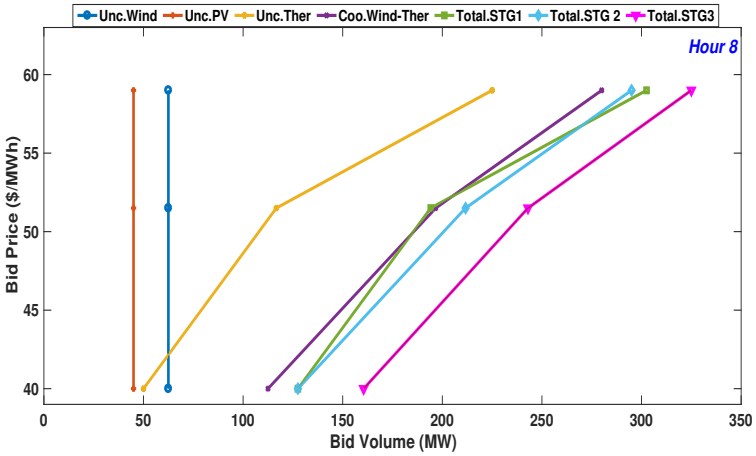

(b) Multi-objective bidding approach

Figure 10: Day-ahead energy market bidding for hour 8

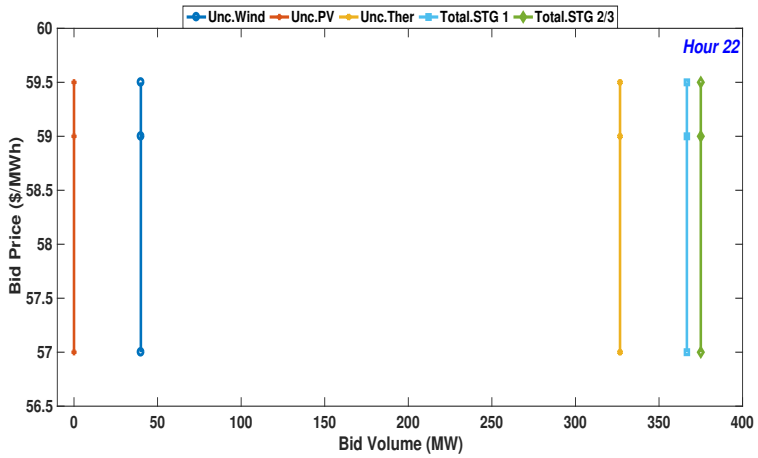

(a) Single objective bidding approach

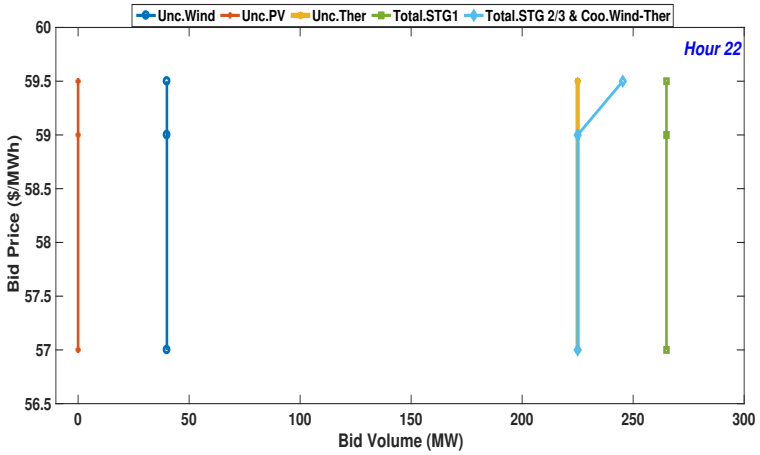

(b) Multi-objective bidding approach

Figure 11: Day-ahead energy market bidding for hour 22

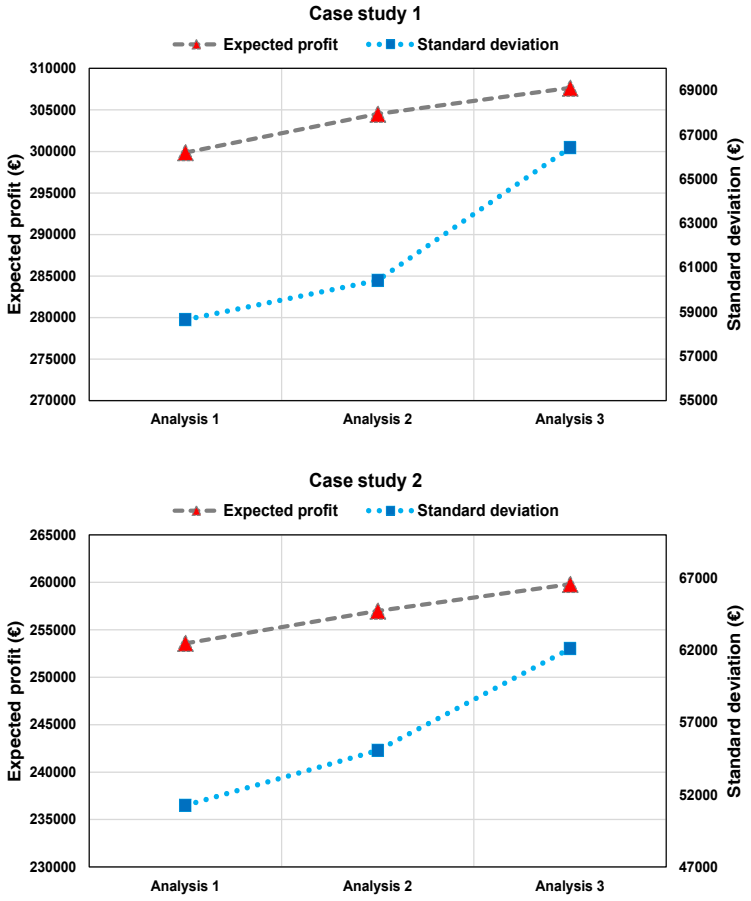

Figure 12: Comparison of expected profit and its standard deviation in various analyses

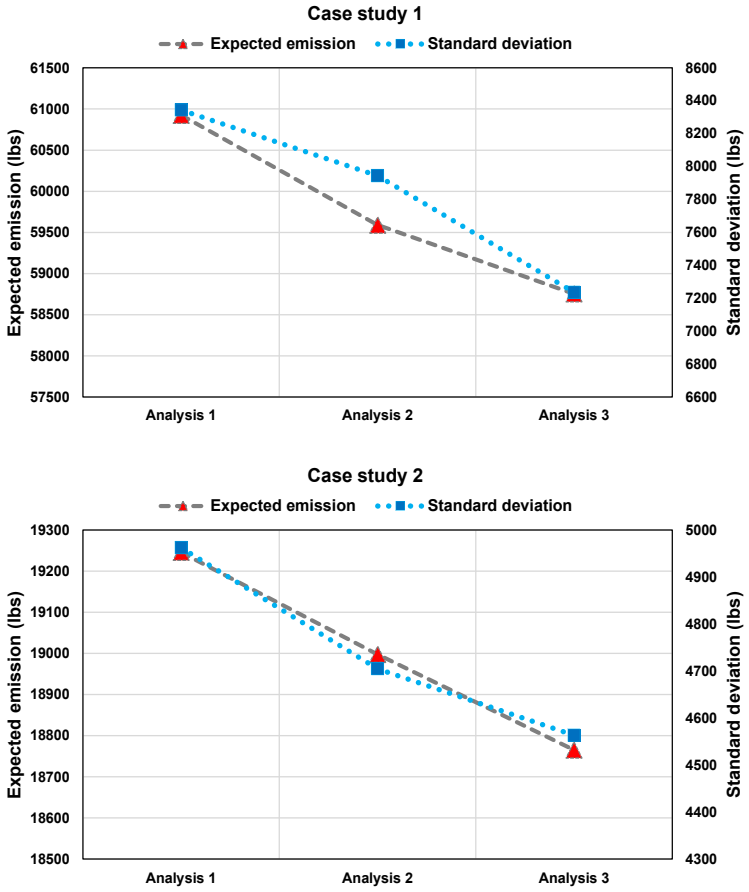

Figure 13: Comparison of expected emission and its standard deviation in various analyses

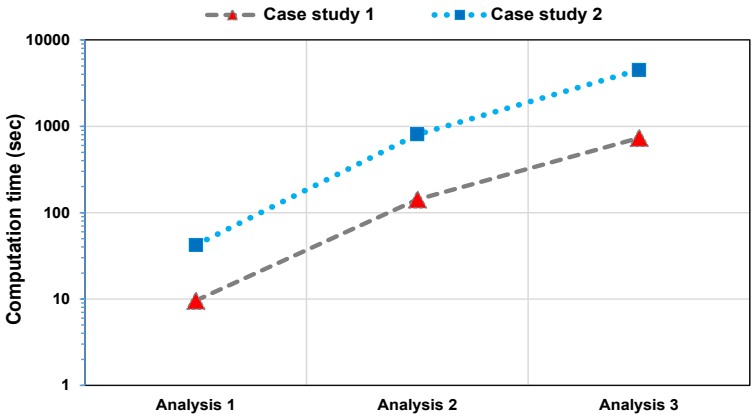

Figure 14: Comparison of computation time in various analyses

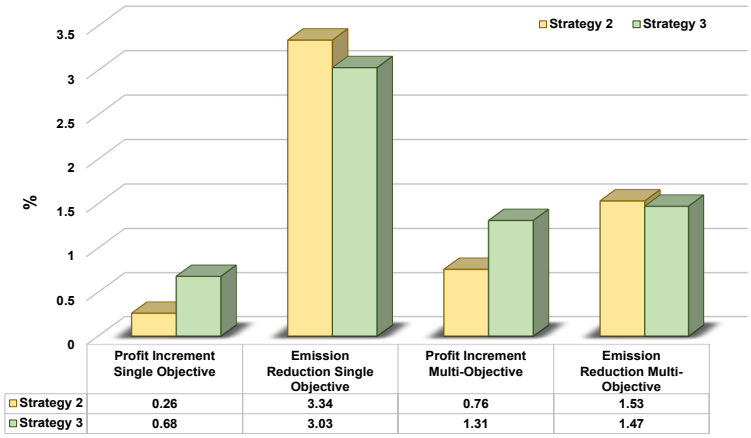

	Profit Increment Single Objective	Emission Reduction Single Objective	Profit Increment Multi-Objective	Emission Reduction Multi-Objective
Strategy 2	0.26	3.34	0.76	1.53
Strategy 3	0.68	3.03	1.31	1.47

(a) Profit increment and emission reduction in both case studies

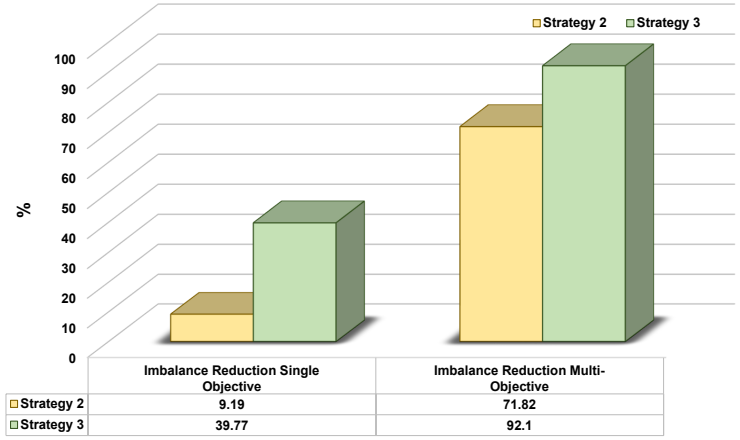

	Imbalance Reduction Single Objective	Imbalance Reduction Multi-Objective
Strategy 2	9.19	71.82
Strategy 3	39.77	92.1

(b) Imbalance reduction in both case studies

Figure 15: Comparison of profit increment, emission and imbalance reductions in the second and third trading strategies

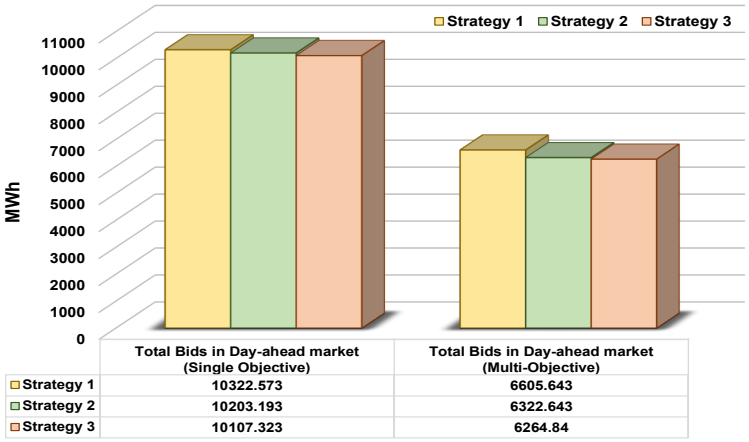

	Total Bids in Day-ahead market (Single Objective)	Total Bids in Day-ahead market (Multi-Objective)
Strategy 1	10322.573	6605.643
Strategy 2	10203.193	6322.643
Strategy 3	10107.323	6264.84

(a) Expected total bids in the day-ahead energy market for both case studies

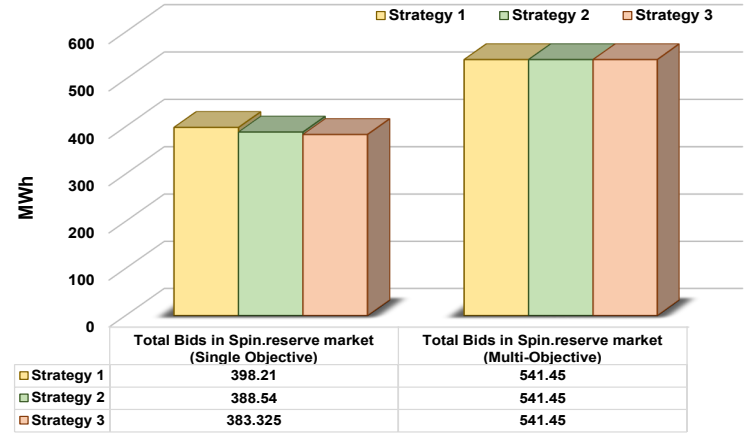

	Total Bids in Spin.reserve market (Single Objective)	Total Bids in Spin.reserve market (Multi-Objective)
Strategy 1	398.21	541.45
Strategy 2	388.54	541.45
Strategy 3	383.325	541.45

(b) Expected total bids in the spinning reserve market for both case studies

Figure 16: Comparison of expected total day-ahead energy and spinning reserve bids in different trading strategies

Table 1: Taxonomy of the reviewed papers

Ref.	Combination of Various Energy Sources	Problem Type	Uncertain Parameters					Uncertainty Modeling	Objective Functions	Solution Methodology of MOP
			EM	SPRM	BM	REP	OS			
[7]	Large consumer	BS	√	—	—	√	√	SP-RO	CSM	—
[8]	Large consumer	BS	√	—	—	√	√	SP-RO	CSM	—
[9]	Microgrid	SS	√	√	—	√	√	SP	CSM	—
[10]	Industrial Plant	SS	—	—	—	—	—	—	CSM	—
[11]	Thermal	SS	√	√	—	√	√	PP	PFM	—
[12]	Large consumer	SS	—	—	—	—	—	—	CSM+ICM	WSM
[13]	VPP	SS	√	√	—	√	√	SP	PFM	—
[14]	Wind-PSP	SS	—	—	—	√	—	SP	PFM	—
[15]	Hydro-thermal	SS	√	√	—	—	√	SP	PFM	—
[16]	Wind-thermal	BS	√	—	—	√	—	SP	PFM	—
[17]	Wind-thermal	SS	—	—	√	—	—	—	PFM	—
[18]	Wind-thermal	BS	√	—	—	√	—	SP	PFM	—
[19]	Wind-thermal-PSP	BS	√	—	√	√	√	SP	PFM	—
[20]	Microgrid	SS	—	—	√	—	—	—	CSM+EMM	EPM
[21]	Hydro-thermal	SS	—	—	—	—	—	—	PFM+EMM	EPM
[22]	Hydro-thermal-PSP	EED	—	—	—	—	√	SP	CSM+EM	NBIM
This paper	**Wind-thermal-PV**	**BS**	√	√	√	√	—	**SP**	**PFM+EMM**	**WSM+FSA**

Note : EM-Energy market; SPRM-Spinning reserve market; BM-Balancing market; REP-Renewable production; OS-Other sources; MOP-Multi-objective programming; PSP-Pumped storage Plant; VPP-Virtual Power Plant; MG-Microgrid; PV-Photovoltaic; BS-Bidding strategy; SS-Self-Scheduling; EED-Economic emission dispatch; SP-Stochastic programming; RO-Robust optimization; PP-Probabilistic possibilistic; PFM-Profit maximization; CSM-Cost minimization; EMM-Emission minimization; ICM-Investment cost minimization;WSM-Weighted sum method; WSM+FSA-Weighted sum method+Fuzzy satisfying approach; EPM-Epsilon Constraint method; NBIM-Normal boundary intersection method

Table 2: Thermal units information

Thermal Units	Cost coefficients of generator			P_{min} (MW)	P_{max} (MW)
	a_g(€/MW^2h)	b_g(€/MWh)	c_g(€/h)		
G1	0.0144	31.400	40.260	0	50
G2	0.0339	43.022	85.509	5	45
G3	0.0339	42.022	82.342	5	45
G4	0.0330	28.090	42.760	25	100
G5	0.0248	26.504	49.140	25	100

Table 3: Technical specification of thermal units

Thermal units	RDR(g) (MW/hr)	RUR(g) (MW/hr)	STDRL(g) (MW/hr)	STURL(g) (MW/hr)	STUC(g) (€)
G1	50	50	30	20	0
G2	15	15	20	15	88
G3	15	15	20	15	88
G4	50	50	60	50	110
G5	50	50	60	50	110

Table 4: Emission coefficients of thermal units

Thermal units	Coefficient of SO_2 emission function			Coefficient of NO_x emission function		
	α_g (lbs/MW^2)	β_g (lbs/MW)	γ_g (lbs)	α_g (lbs/MW^2)	β_g (lbs/MW)	γ_g (lbs)
G1	0.0249	3.554	1.866	0.0087	1.345	3.716
G2	0.0167	12.259	4.470	0.0073	5.945	5.298
G3	0.0167	11.259	4.470	0.0073	5.945	5.298
G4	0.0157	2.762	2.262	0.0095	0.820	4.653
G5	0.0157	2.762	2.262	0.0095	0.820	4.653

Table 5: Information on wind turbines and PV site

Parameter	Value	unit	Parameter	Value	unit
v_{ci}	3	m/s	η^{PV}	15	%
v_r	15	m/s	S^{PV}	10^6	m^2
v_{co}	25	m/s	P^{PV}_{rated}	150	MW
P^{W}_{rated}	250	MW	-	-	-

Table 6: Results of single objective bidding strategy in various trading strategies

Trading strategy	Expected profit (€)	Expected emission (lbs)	Imbalance cost (€)
Wind uncoordinated	94868.919	—	16995.914
PV uncoordinated	53734.278	—	8373.622
Thermal uncoordinated	153831.439	61455.848	—
Sum uncoordinated wind and thermal	248700.358	61455.848	16955.914
Coordinated wind and thermal	249486.914	59401.666	14663.655
Sum uncoordinated wind, PV and thermal (Strategy 1)	302434.636	61455.848	25369.536
Sum uncoordinated PV and coordinated wind-thermal (Strategy 2)	303221.192	59401.666	23037.277
Coordinated wind, PV and Thermal (Strategy 3)	304509.778	59590.001	15278.357

Table 7: Results of Multi-objective bidding strategy in various trading strategies

Trading strategy	Expected profit (€)	Expected emission (lbs)	Imbalance cost (€)
Wind uncoordinated	94868.919	—	16995.914
PV uncoordinated	53734.278	—	8373.622
Thermal uncoordinated	105035.729	19266.137	—
Sum uncoordinated wind and thermal	199904.648	19266.137	16955.914
Coordinated wind and thermal	201832.005	18971.043	-1225.947
Sum uncoordinated wind, PV and thermal (Strategy 1)	253638.926	19266.137	25369.536
Sum uncoordinated PV and coordinated wind-thermal (Strategy 2)	255566.283	18971.043	7147.675
Coordinated wind, PV and Thermal (Strategy 3)	256978.704	18997.492	2003.541

Table 8: Results of emission quota arbitraging for Pareto optimal solutions of strategy 3

Total Emission (lbs)	Profit without emission trade (€)	Emission trades (lbs)	Net profits (€)			
			λ^{EM}=0.1 (€/lbs)	λ^{EM}=0.3 (€/lbs)	λ^{EM}=0.5 (€/lbs)	λ^{EM}=1 (€/lbs)
59590.001	304509.778	-39590.001	**300550.778**	292632.778	284714.778	264919.777
56009.132	304058.522	-36009.132	300457.608	293255.782	286053.956	268049.390
52814.999	303192.137	-32814.990	299910.637	**293347.637**	286784.638	270377.147
49652.657	301854.928	-29652.657	298889.662	292959.131	287028.600	272202.271
46939.804	300526.825	-26939.804	297832.845	292444.884	**287056.923**	273587.021
42807.933	297896.198	-22807.933	295615.405	291053.818	286492.232	275088.265
38700.833	294798.142	-18700.833	292928.059	289187.892	285447.726	276097.309
35374.524	291777.572	-15374.524	290240.120	287165.215	284090.310	**276403.048**
31145.031	287088.975	-11145.031	285974.472	283745.466	281516.460	275943.944
28286.335	283176.988	-8286.335	282348.355	280691.088	279033.821	274890.653
25544.215	277774.429	-5544.215	277220.008	276111.165	275002.322	272230.214
22952.056	270843.444	-2952.056	270548.238	269957.827	269367.416	267891.388
21044.007	264561.387	-1044.007	264456.986	264248.185	264039.384	263517.380
18997.492	256978.704	1002.508	257078.955	257279.456	257479.958	257981.212
14221.486	236828.236	5778.514	237406.087	238561.790	239717.493	242757.218
12567.015	229008.445	7432.985	229751.744	231238.341	232724.938	236441.430
8303.996	206041.240	11696.004	207210.840	209550.041	211889.242	217737.244
0	149735.991	20000.000	151735.991	155735.991	159735.991	169735.991